

## Effects of mixing protocol on morphology and properties of PA6/ABS blends compatibilized with MMA-MA

L.D.C. Castro,<sup>1</sup> A.D. Oliveira,<sup>1</sup> M. Kersch,<sup>2</sup> V. Altstädt,<sup>2</sup> L.A. Pessan<sup>1</sup>

<sup>1</sup>Department of Materials Engineering, Federal University of São Carlos, via Washington Luiz, Km 235, 13565-905, São Carlos SP, Brazil

<sup>2</sup>Department of Polymer Engineering, Faculty of Engineering Science, University of Bayreuth, Bayreuth, 95447, Germany  
Correspondence to: L. D. C. Castro (E-mail: lucasdanielcastro@hotmail.com)

**ABSTRACT:** The effect of different mixing protocols in the preparation of PA6/ABS/MMA-MA (57.5/37.5/5 wt %) blends on their morphological, rheological, thermal, thermomechanical, and mechanical behavior were studied. Despite the second-phase size reduction due to copolymer incorporation, mixing sequence seems to play an important role in the properties of the blends. When PA6 is blended with the pre-blended ABS/MMA-MA system, compatibilizer is preferentially located in ABS phase and a co-continuous structure is formed. The co-continuity is believed to be responsible for the enhancements in toughness, but excessive presence of MMA-MA in ABS phase seems to hamper thermomechanical properties. On the other hand, when ABS is blended with the PA6/MMA-MA system previously prepared, compatibilizer is preferentially located in PA6 phase and a particle-in-matrix morphology is observed. The absence of excessive amount of MMA-MA in ABS phase avoids the negative effect on thermomechanical resistance, however enhancements in toughness are not so pronounced. © 2016 Wiley Periodicals, Inc. *J. Appl. Polym. Sci.* **2016**, *133*, 43612.

**KEYWORDS:** blends; compatibilization; polyamides; structure–property relations

Received 20 January 2016; accepted 6 March 2016

DOI: 10.1002/app.43612

### INTRODUCTION

Polyamides are in the major class of engineering polymers due to their good mechanical and thermal properties allied with chemical and wear resistance.<sup>1</sup> However they are notch sensitive; in other words, polyamides are ductile in unnotched state but tend to fail in a brittle manner in presence of a notch. Furthermore, they are also brittle at low temperatures or under severe loading conditions.<sup>2–4</sup> Blending is a well-known method to modify properties of polymeric materials. Among the most common techniques, numerous articles describe the addition of an elastomeric phase as an effective approach to enhance toughness of polyamide-based multiphase systems.<sup>5–10</sup>

Acrylonitrile-butadiene-styrene (ABS) is an engineering thermoplastic which consists of a polybutadiene rubber (PB) phase dispersed into a brittle styrene-acrylonitrile copolymer (SAN) matrix and SAN-graft-PB chains laying on the interface. Despite the complex morphology, ABS is highlighted for good toughness allied with low molding shrinkage and relative low cost, suggesting its use as toughening agent in industrial processes.<sup>11</sup>

Blends based on PA6/ABS systems are of commercial interests due to their excellent stiffness/toughness balance and competitive cost.<sup>12</sup> Nonetheless, most polymer pairs, including PA6/ABS, are

thermodynamically immiscible and incompatible because of unfavorable molecular interactions between constituents. This leads to large interfacial tension in melt state, hampering the proper dispersion of the second phase and allowing morphological rearrangements during low stress or quiescent conditions. Furthermore, unfavorable interactions are also responsible for poor interfacial adhesion in solid state resulting in inferior mechanical properties.<sup>13–16</sup> Enhancement of interaction of components can be promoted by addition of conveniently chosen polymeric species to incompatible polymer blends. An adequate compatibilization process reduces the interfacial tension and retards coalescence of the dispersed phase via steric stabilization resulting in a finer and more stable morphology. Additionally, adhesion between phases is also improved and, thus, reduces the possibility of interfacial defects.<sup>17–19</sup>

Among several methods reported in literature, the preferred strategy to compatibilize PA6/ABS systems has been incorporating a functional copolymer which is miscible with SAN phase of ABS and also capable of chemically interact with amine (NH<sub>2</sub>) groups of polyamide through *in situ* reactions during melt blending process.<sup>13,14</sup> In a previous work, Araujo *et al.*<sup>20</sup> demonstrated the utility of methyl methacrylate-co-maleic anhydride (MMA-MA) as compatibilizer for PA6/ABS. This copolymer contains maleic



Figure 1. Employed twin-screw profile.

anhydride (MA) groups capable of reacting with polyamide end groups whereas the methyl methacrylate (MMA) has been demonstrated to be miscible with the SAN phase of ABS over a range of AN contents.<sup>21</sup>

Nevertheless, the ternary PA6/ABS/MMA-MA blend, as other polymeric mixtures, shows an interesting and noteworthy problem. Generally speaking, mixing protocol can influence the morphology and performance of multi-component systems.<sup>22,23</sup> In previous studies Kim *et al.*<sup>13</sup> have investigated the blending sequence effect on dynamical mechanical, rheological and morphological properties of ABS/SMA/nylon-6 ternary blends. The authors reported that when nylon-6 was blended with the pre-blended ABS/SMA (90/10), the SMA-g-nylon6 formed by *in situ* reactions seemed to lie at interfacial region and act as an effective compatibilizer. However the SMA-g-nylon-6 lies preferentially in the nylon-6 domain, improving the thermal resistance and modulus, when ABS was blended with the pre-blended SMA/nylon-6 (10/90). Ha *et al.*<sup>23</sup> have studied the effect of the blending sequence in PP/mPE/HDPE ternary blends and reported that, regardless of mixing sequence, mPE encapsulated HDPE in the PP matrix. Moreover, the best mechanical properties were generally obtained with premixing of mPE/HDPE followed by mixing with PP. Hale *et al.*<sup>24</sup> reported that fracture properties depend on the order of mixing of the blend components in PBT/ABS/MGE blends. According to the authors, mixing all components together in a single-pass extrusion improves low-temperature toughness but reduces impact strength at room-temperature compared to uncompatibilized blends. Nonetheless, in a two-pass method where PBT/MGE are pre-blended prior to incorporating ABS in a second extrusion, room-temperature impact strength is superior to the one prepared by the single-pass method. Finally, when a two-pass method is used where ABS/MGE are premixed prior to extrusion with PBT, the impact properties at all temperatures are inferior when compared to uncompatibilized blends.

In this present work MMA-MA was incorporated in PA6/ABS system as a compatibilizer. As shown above, different blending protocols may alter the order of chemical reactions and location of graft copolymer formed *in situ*, modifying the interfacial region which is the main responsible for blend performance. Thus, the focus of this study is to investigate the mixing sequence influence in morphological, rheological, thermal, thermomechanical and mechanical properties of PA6/ABS/MMA-MA ternary blends.

## EXPERIMENTAL

Polyamide 6 (PA6) commercially known as B300 and supplied by Polyform (density  $1.13 \text{ g cm}^{-3}$ , MFI  $2.9 \text{ g } 10 \text{ min}^{-1}$  at  $230 \text{ }^\circ\text{C}$  and  $2.16 \text{ kg}$ ) was used as the matrix phase. Acrylonitrile-butadiene-styrene (ABS) commercialized as Cyclic Resin EX58 (52.8 wt % butadiene, 12.4 wt % acrylonitrile, and 34.6 wt % styrene) was kindly donated by SABIC and used as dispersed phase.

The copolymer methyl methacrylate-co-maleic anhydride (MMA-MA) with 3 wt % of maleic anhydride was obtained by solution polymerization using dimethyl sulfoxide (DMSO) as solvent and azobisisobutyronitrile (AIBN) as reaction initiator. Methyl methacrylate (MMA) and maleic anhydride (MA) were employed as monomers and ethyl acrylate (EA) as auxiliary comonomer to increase stability of the copolymer against unzipping at processing temperatures.<sup>20</sup> All the monomers were supplied by Sigma Aldrich and used as received without prior purification. The synthesis was carried out in a reactor under intensive mixing at  $70 \text{ }^\circ\text{C}$  and inert nitrogen atmosphere for 5 h. Subsequently, the product obtained was precipitated in methanol to remove all nonreacted DMSO and MA. After separation and filtration, the MMA-MA was dried in a forced air circulation oven at  $50 \text{ }^\circ\text{C}$  for 24 h. The synthesis procedure used in this study was based on similar techniques previously reported in literature.<sup>25,26</sup>

The polymeric mixtures were prepared in a co-rotating twin-screw extruder manufactured by B&P Process Equipment and Systems ( $L/D = 25$ ,  $D = 19 \text{ mm}$ ), with temperature profile of  $200/220/220/220/230 \text{ }^\circ\text{C}$  operating at screw speed of 160 RPM. The twin-screw profile used during melt blending process can be observed in Figure 1.

Prior to each melt processing step, all polyamide-containing material were dried in a vacuum oven at  $80 \text{ }^\circ\text{C}$  for at least 16 h. Two different blending protocols were used to prepare ternary blends, according to the following procedure:

- (PA6/MMA-MA)+ABS: PA6 and MMA-MA were preblended in the first extrusion step. Subsequently the obtained product was blended with ABS in a second extrusion step.
- (ABS/MMA-MA)+PA6: ABS and MMA-MA were preblended in the first extrusion step. Subsequently the obtained product was blended with PA6 in a second extrusion step.

The composition of both compatibilized blends was fixed as PA6/ABS/MMA-MA (57.5/37.5/5 wt %). For reference a PA6/ABS (60/40 wt %) binary blend was also prepared in a single extrusion step. The materials obtained by extrusion were quenched in water, granulated, dried and injection molded at  $245 \text{ }^\circ\text{C}$  using an Arburg Allrounder 270V machine with mold temperature of  $50 \text{ }^\circ\text{C}$  into standard specimens for mechanical and thermomechanical analysis.

Evidences of *in situ* reactions between PA6 and MMA-MA were investigated using a Haake torque rheometer equipped with roller rotors operating at  $260 \text{ }^\circ\text{C}$  and 60RPM for 10 min.

Morphologies of the materials were determined by TEM using a Magellan 400L scanning electron microscope operating in transmission mode. The samples were cryomicrotomed in ultrathin sections from Izod bars, perpendicular to the flow direction, using a Reichert-Jung Ultracut E type microtome equipped with a diamond knife. A two-step selective staining technique was

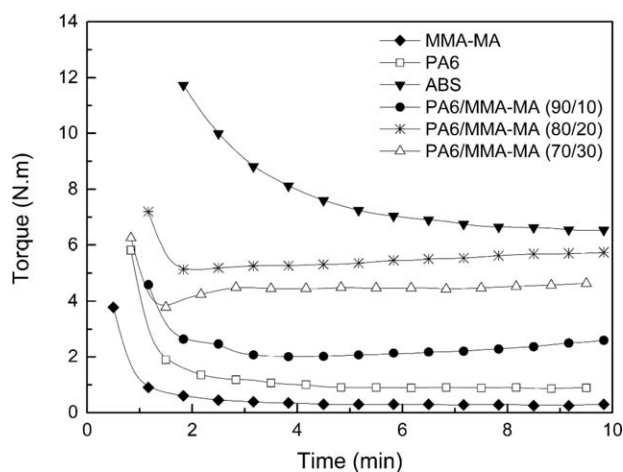


**Figure 2.** Torque-time curves for MMA-MA, PA6, ABS and PA6/MMA-MA in various compositions.

used to generate the phase contrast in which the sections were exposed to osmium tetroxide vapor ( $\text{OsO}_4$ ) for 15 h and posteriorly to ruthenium tetroxide vapor ( $\text{RuO}_4$ ) for 2 h to respectively stain the PB and SAN phases.

Viscoelastic properties were measured on an Advanced Rheometric Expansion System (ARES) equipped with 20 mm diameter parallel plates. Samples were compression molded in 1 mm thick disks at 245 °C. Frequency sweeps from 500 to 0.1  $\text{rad s}^{-1}$  were carried out in oscillatory shear using a strain of 5% at 245 °C under dry nitrogen atmosphere. All the rheological measurements were performed within the linear viscoelastic region of the materials.

Melting and crystallization behavior was evaluated by differential scanning calorimetry (DSC) using a DSC Q100 equipment (TA Instruments). Samples were obtained directly from extruded granules and subjected to heating-cooling-heating cycles from 30 °C to 250 °C with constant rate of 10 °C  $\text{min}^{-1}$  under nitrogen atmosphere. Crystallization temperatures ( $T_c$ ) and crystallization enthalpies ( $\Delta H_c$ ) were obtained from cooling cycles; melting points ( $T_m$ ) and melting enthalpies ( $\Delta H_f$ ) were obtained from second heating thermograms and the degree of crystallization ( $X_c$ ) were calculated according to eq. (1):

$$X_c = \frac{\Delta H_f}{\Delta H_f^0(\text{PA6})} \times \frac{1}{w_{\text{PA6}}} \times 100 \quad (1)$$

where  $\Delta H_f$  is the fusion enthalpy obtained by the second heating cycle;  $\Delta H_f^0(\text{PA6}) = 190.8 \text{ J g}^{-1}$ <sup>27</sup> is the fusion enthalpy of 100% crystalline PA6 and  $w_{\text{PA6}}$  is the weight fraction of PA6.

Heat deflection temperatures (HDT) were measured according to ASTM D648 using a CEAST equipment model HDT 6 VICAT P/N 6921.000 under outer fiber stress of 1.82 MPa (Method A) and heating rate of 120 °C  $\text{h}^{-1}$ .

Tensile properties were measured according to ASTM D638 (type I) in an Instron machine model 5569 at a crosshead speed of 5  $\text{mm min}^{-1}$ . Notched Izod impact measurements were made at room temperature using a CEAST Resil 25 pendulum-type impact tester according to ASTM D256. All mechanical and thermomechanical analysis were carried out using dry-as-molded specimens.

## RESULTS AND DISCUSSION

### MMA-MA Reactivity

Melt viscosities of nonreactive mixtures can be roughly approximated by a weight average of the viscosities of individual components. However, in reactive systems positive deviations from simple additivity are expected as chemical reactions proceed.<sup>28</sup> In general, the formation of grafts, branches or crosslinking during melt blending process can be correlated with increases in the overall molecular weight of reacting polymeric systems, leading to increments in melt viscosities.<sup>28,29</sup> Thus, one can indirectly follow the progress of *in-situ* reactions by simply monitoring the viscosity response during melt processing.<sup>30</sup> Figure 2 shows the torque response with time for MMA-MA, PA6, ABS, and PA6/MMA-MA mixtures with different MMA-MA concentrations.

According to Figure 2, the torque of PA6/MMA-MA (90/10) is significantly higher than the ones obtained for neat components; this is a clear evidence that *in-situ* reactions between PA6 amide groups and MMA-MA maleic anhydride groups, known as imidization, might be occurring. The imidization scheme is illustrated by Figure 3.

A posterior increment in MMA-MA content to 20 wt % is followed by a corresponding increasing in torque, indicating the formation of higher PA6-g-MMA amount. However, it is observed in the mixture with 30 wt % of MMA-MA in which the torque decreases when compared to the (80/20) curve. The explanation could be based on the existence of a hypothetical limit number of *graft* reactions, which might be direct related to the amount of amine groups available to chemically react. This is a valuable information, suggesting that is not necessary huge amounts of MMA-MA to assure the compatibilization process. Once such hypothetical limit, which could be dependent on the experimental conditions, is reached, there will be too few  $\text{NH}_2$  groups capable of chemically reacting. Thus, the incorporation of additional MMA-MA will just act as a plasticizer, reducing the final viscosity of the mixture.

### Morphology

Morphologies of (PA6/ABS) and ternary blends are presented in Figure 4. According to Figure 4(a), the non-compatible system shows a rough morphology constituted by large and highly heterogeneous ABS domains. Among many factors, the second-phase stratification is mostly related to the large viscosity difference between the two components. With a higher viscosity of dispersed phase (ABS) a fine break-up would be more difficult.<sup>13</sup>

Regardless of the employed blending protocol, it is possible to observe that the incorporation of MMA-MA can promote a

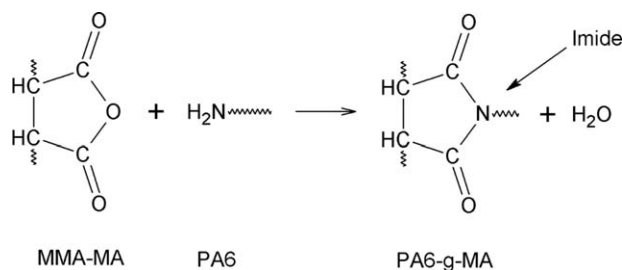


**Figure 3.** Imidization scheme.

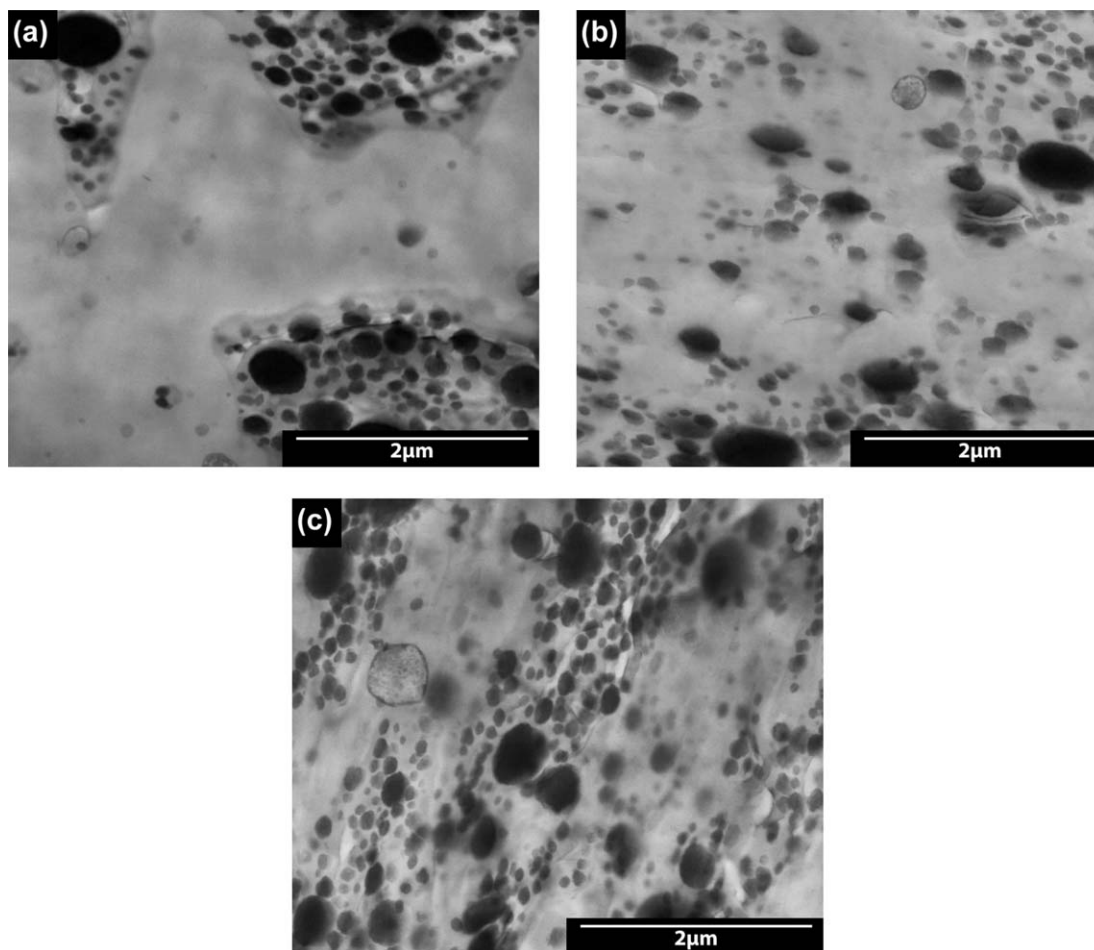


**Figure 4.** TEM photomicrographs of (a) (PA6/ABS); (b) (PA6/MMA-MA)+ABS, and (c) (ABS/MMA-MA)+PA6.

significant reduction of ABS particle size. It has been extensively shown that presence of conveniently chosen polymeric species, normally functionalized copolymers, leads to a reduction in dispersed particle size. This reduction is mainly attributed to the efficiency of these copolymers in promoting steric stabilization of second phase, suppressing the coalescence phenomena.<sup>31–33</sup> Furthermore, an effective compatibilizer system also improves the adhesion between phases, resulting in superior mechanical properties.<sup>18</sup>

The morphology of (PA6/MMA-MA)+ABS shown in Figure 4(b) is a particle-in-matrix structure in which ABS is finely and homogeneously dispersed in the PA6 matrix. On the other hand, the (ABS/MMA-MA)+PA6 presented in Figure 4(c) shows elongated ABS domains which are apparently interconnected, forming an almost co-continuous structure. The difference between (PA6/MMA-MA)+ABS and (ABS/MMA-MA)+PA6 morphologies is probably caused by the combined effect of viscosity approach and compatibilizing effect of PA6-g-MMA-MA.

As mentioned earlier, MMA-MA can react “*in situ*” with PA6. During melt blending of (PA6/MMA-MA)+ABS, the copolymer is obviously very inclined to chemically interact with PA6, favoring the formation of PA6-g-MMA-MA. As verified in torque rheometry curves (Figure 2), the grafted-copolymer shows much

higher viscosity values compared to neat polyamide due to the imidization reaction. Once viscosity of ABS is also higher than PA6, it is expected that viscosity ratio of PA6-g-MMA-MA/ABS, is closer to unity when compared to the value concerning to PA6/ABS pair. With the viscosity ratio of the components at least closer to unity, a finer break-up of dispersed phase would be expected.<sup>13</sup> On the other hand, in (ABS/MMA-MA)+PA6 the copolymer is preferentially located in the ABS phase and, for consequence, the imidization reaction should occur in a smaller degree. Possibly this situation results in a viscosity ratio of PA6 to ABS close to the volumetric ratio, which according to Paul Barlow model,<sup>34</sup> is the main criterion to obtain co-continuity. Since there is “*in-situ*” graft reactions occurring during the blending steps, the viscosity ratio quantification is not trivial and further and extensive specific investigations would be needed. Furthermore, torque rheometry analysis allied with TEM micrographics provided valuable information, supporting the proposed mechanism.

#### Rheological Properties

Rheological behavior of multiphase systems is strongly influenced by morphology which is determined by several parameters such as composition, viscosity of each component and interfacial tension. The influences of MMA-MA incorporation

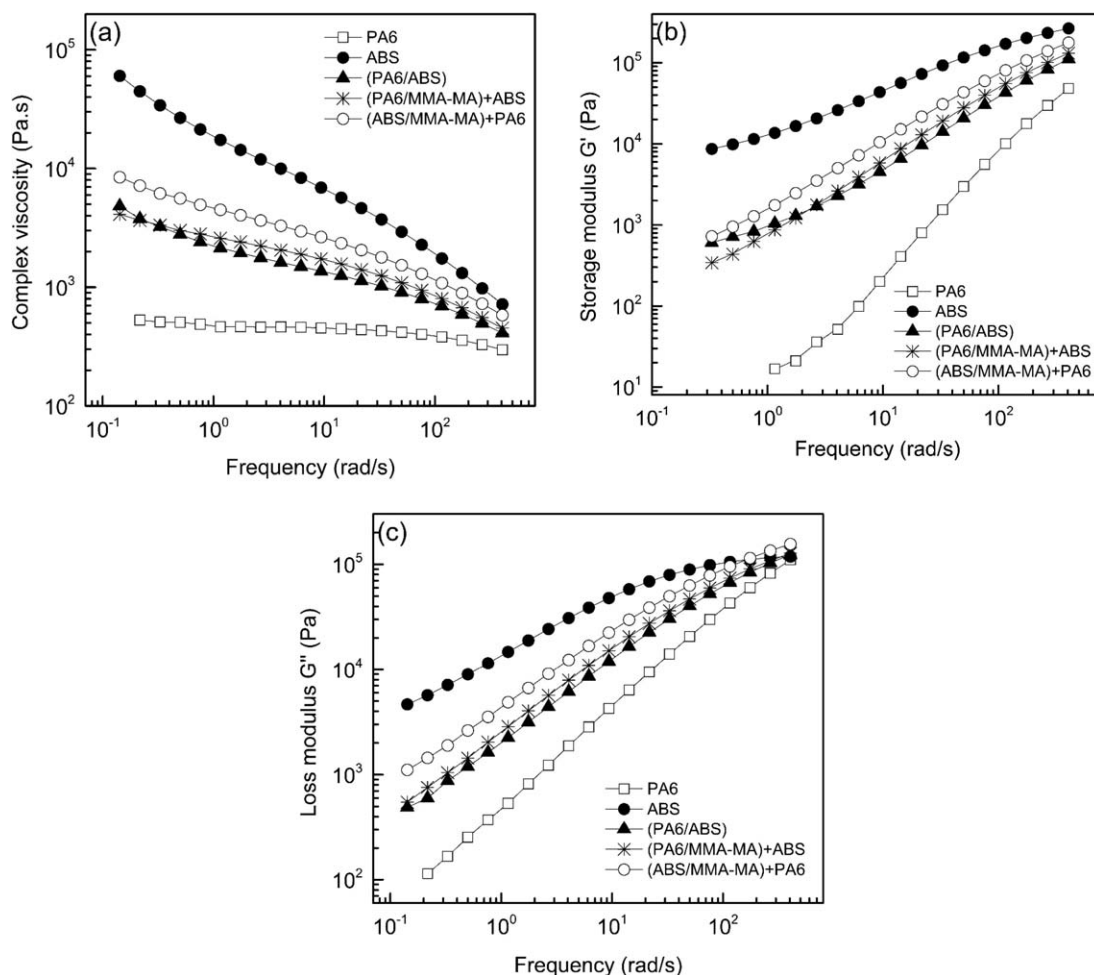


**Figure 5.** Rheological behavior of PA6, ABS, (PA6/ABS), and ternaryblends (a) complexviscosity; (b) storage modulus ( $G'$ ) and (c) loss modulus ( $G''$ ).

and blending sequence on the rheological properties are shown in Figure 5.

According to Figure 5(a) one can notice that binary and ternary blends show complex viscosities between the constituent components. However, it can be observed the incorporation of MMA-MA increased the viscosities of both compatibilized systems compared to (PA6/ABS). This effect, which is more pronounced in intermediate frequencies, is possibly related to the enhancement in the interfacial interaction due to the grafting reaction between MA and the amino end groups of PA6. When the interface is strong, the deformation of dispersed phase is efficiently transferred along the structure, resulting in higher complex viscosities and better compatibility between phases.<sup>11</sup>

Regarding the blending sequence, is possible to observe a quite different rheological behavior of (ABS/MMA-MA)+PA6 compared to (PA6/MMA-MA)+ABS. Especially at low frequencies, the first one shows a significant increase in viscosity. This effect is normally attributed to the existence of a co-continuous structure which, according to Jafari *et al.*,<sup>12</sup> can be explained by extra stresses connected with the shape relaxation. As shown by Figure 5(b,c), the same behavior exist for both storage modulus  $G'$  and loss modulus  $G''$ . At low frequencies, both  $G'$  and  $G''$  of (ABS/MMA-MA)+PA6 are higher than (PA6/MMA-MA)+ABS.

This effect is much more pronounced in the elastic properties, clearly visible in storage modulus curves, and also attributed to its almost co-continuous structure.<sup>11,12</sup>

### Thermal Properties

Despite the rubber phase dispersion and its coupling to the matrix are the dominant issues in toughening of PA6, it must be considered that polyamides are semi-crystalline materials whose nature might be influenced by the blending sequence process and any associated chemistry.<sup>30</sup>

Melting and crystallization behavior of PA6 component in blends were analyzed by DSC. The DSC characteristic data is summarized in Table I and the thermograms are shown in Figure 6. The DSC thermograms shown in Figure 6(b) reveals bimodal melting peaks for all compositions during the second heating cycle. According to literature,<sup>35,36</sup> the double melting endotherm is related to the polymorphism of polyamide 6, which consists in the coexistence of  $\gamma$  and  $\alpha$  crystalline forms with melting temperatures of 212 °C and 220 °C, respectively.

From Table I is possible to observe that the PA6 crystallization degree is reduced by ABS presence. This behavior was previously reported by Bhardwaj *et al.*<sup>37</sup> and probably is related to the retardation of homogenous nucleation process of polyamide

**Table I.** Effect of MMA-MA Incorporation and Blending Sequence on the Melting and Crystallization Parameters of PA6, (PA6/ABS) and Ternary Blends

Samples	Cooling		Second heat				$X_c$ (%)
	$T_c^a$ (°C)	$\Delta H_c^b$ (Jg <sup>-1</sup> )	$T_{m1}^c$ (°C)	$T_{m2}^d$ (°C)	$T_{m3}^e$ (°C)	$\Delta H_m$ (Jg <sup>-1</sup> )	
PA6	188	70	-	215	222	67	35
(PA6/ABS)	188	39	-	216	222	37	32
(PA6/MMA-MA)+ABS	186	34	-	215	222	31	28
ABS/MMA-MA)+PA6	186	37	207	214	221	34	31

<sup>a</sup>Crystallization temperature.<sup>b</sup>Crystallization enthalpy.<sup>c</sup>Melting temperature of less stable  $\alpha$ -phase.<sup>d</sup>Melting temperature of  $\gamma$ -phase.<sup>e</sup>Melting temperature of  $\alpha$ -phase.

6 during its crystallization in blend. Despite the fact that it hardly affects the melting temperatures, one can notice that the ABS incorporation intensifies the melting peak in  $T_{m2} = 216^\circ\text{C}$ , changing the proportion between  $\alpha$  and  $\gamma$  phases. In general, the addition of MMA-MA slightly reduces the degree of crystallization and crystallization temperature of the ternary blends compared to (PA6/ABS). In a similar way as ABS incorporation, this behavior can be attributed to disturbances in homogeneous nucleation process of PA6 due to the copolymer presence. Moreover, the MMA-MA incorporation does not seem to affect the melting temperatures, which are almost the same for reactive and nonreactive systems.

Regarding to the mixing protocol, a considerable difference between the melting thermograms of ternary blends can be observed. From Figure 6(b), it is observed that the  $\gamma$ -peak of (ABS/MMA-MA)+PA6 is a little bit more pronounced compared to (PA6/MMA-MA)+ABS, suggesting the mixing sequence might slightly affect the proportion between  $\alpha$  and  $\gamma$  phases. Furthermore, besides the most evident peaks at  $T_{m2}$  and  $T_{m3}$ , the (ABS/MMA-MA)+PA6 curves exhibit a shoulder at  $T_{m1} = 207^\circ\text{C}$  which is inexistent in (PA6/MMA-MA)+ABS and probably is related to the formation of a less stable crystalline  $\alpha$ -phase.<sup>38</sup>

Still from Table I it is also possible to verify that the blending sequence does not seem to play an important role in the melting temperatures, since the values are almost the same for both ternary blends. However, an interesting behavior concerning the crystallization can be noticed. Apparently the blending sequence might affect the degree of crystallization of compatibilized systems. In the (ABS/MMA-MA)+PA6 the MMA-MA is expected to be preferentially located in the ABS phase, reducing its negative influence in the crystallization process of PA6 and, thus, resulting in higher crystallinity. On the other hand, in (PA6/MMA-MA)+ABS system the PA6-g-MMA-MA formation is probably favored, hampering the homogeneous nucleation of PA6 and leading to lower degree of crystallization value.

### Thermomechanical and Mechanical Properties

Table II summarizes the thermomechanical and mechanical properties of neat components, binary, and ternary blends. The thermomechanical performance of materials was evaluated by heat distortion temperature (HDT). According to Table II it is clear that ABS incorporation can dramatically enhance the thermomechanical resistance of PA6, once all blends exhibits higher HDT values compared to neat polyamide. The utility of ABS in improving the heat distortion temperature of semi-crystalline

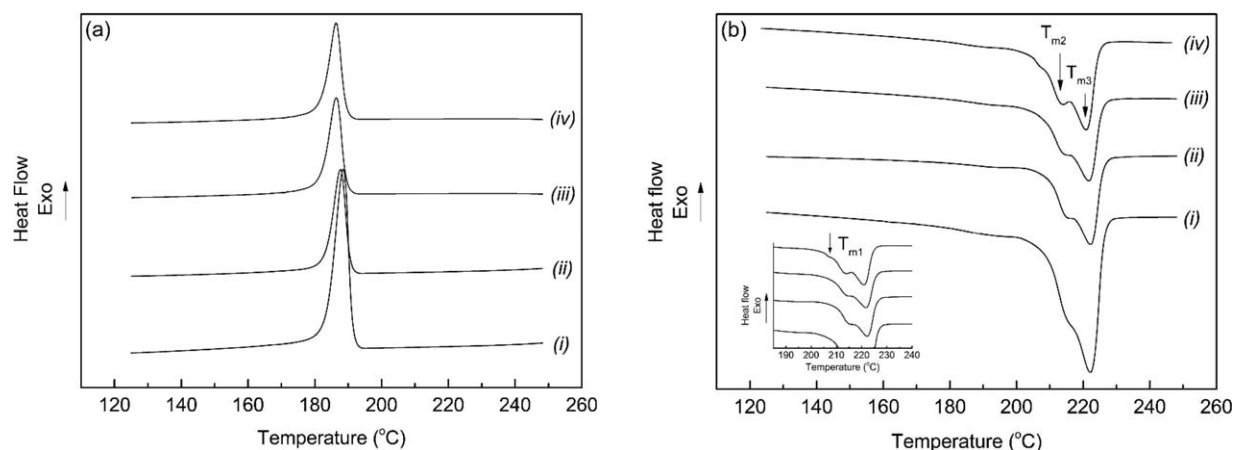


**Figure 6.** DSC thermograms obtained during (a) first cooling cycle and (b) second heating cycle of (i) PA6; (ii) (PA6/ABS); (iii) (PA6/MMA-MA)+ABS and, (iv) (ABS/MMA-MA)+PA6.

**Table II.** Thermomechanical and Mechanical Properties of PA6, ABS, (PA6/ABS), and Ternary Blends Prepared by Different Blending Sequences

Sample	HDT(°C)	Izod impact (Jm <sup>-1</sup> )	Modulus (GPa)	Yield stress (MPa)	Elongation at break (%)
PA6	50 ± 2	40 ± 3	3.06 ± 0.08	77.0 ± 1.8	53 ± 4
ABS	75 ± 3	368 ± 8	2.01 ± 0.06	37.0 ± 1.0	31 ± 4
(PA6/ABS)	71 ± 2	33 ± 3	2.66 ± 0.03	54.0 ± 0.3	9 ± 1
(PA6/MMA-MA)+ABS	70 ± 1	93 ± 3	2.78 ± 0.02	55.4 ± 0.3	67 ± 14
(ABS/MMA-MA)+PA6	62 ± 1	117 ± 3	2.79 ± 0.02	56.1 ± 0.9	141 ± 9

matrix, such as PA6, is mainly attributed to the presence of SAN phase and was previously reported on literature.<sup>29,39</sup>

The simple presence of MMA-MA does not seem to affect the thermomechanical resistance of the blends, as (PA6/MMA-MA)+ABS and (PA6/ABS) shows similar values. In turn, comparing the reactive blends to each other one can obviously conclude that the blending sequence, and consequently the compatibilizer location, plays an important role in HDT. Using the same idea as before, in (ABS/MMA-MA)+PA6 the compatibilizer is expected to be laid preferentially in the ABS phase which is the main phase responsible for the thermomechanical resistance of the blend. The excessive amount of MMA-MA in ABS phase might be hampering its thermomechanical stability, leading to lower HDT values. Furthermore, since the MMA-MA should be preferentially located in PA6 instead of ABS in (PA6/MMA-MA)+ABS, no negative effect in HDT is observed for this composition.

Concerning the mechanical behavior, for all compositions, modulus and yield stress of PA6 decreased with ABS incorporation due to the lower stiffness and strength of the rubber. Furthermore, despite the high toughness of ABS, a dramatically reduction in elongation at break and especially in Izod impact strength of (PA6/ABS) is observed compared to neat polyamide. This reduction in toughness is mainly attributed to the high incompatibility of the system illustrated by second-phase stratification observed by TEM micrographs. Still from Table II, one can notice that a significant enhancement in toughness is achieved by MMA-MA incorporation. Regardless of blending sequence, both (PA6/MMA-MA)+ABS and (ABS/MMA-MA)+PA6 shows higher elongation at break and Izod impact strength values compared to the binary blend. Additionally, a slight increase in modulus is also observed. Is not necessary to mention that, as extensively demonstrated on literature, the presence of conveniently chosen reactive copolymers can reduce the interfacial tension, particle size of dispersed phase and, therefore, sharply enhance toughness of the material.<sup>40,41</sup>

In turn, comparing the ternary blends to each other, a particularly interesting behavior is verified. Contrary to HDT, Izod impact strength and elongation at break values of (ABS/MMA-MA)+PA6 are much higher than the ones obtained for (PA6/MMA-MA)+ABS. At this point is important to recall that mechanical properties, especially toughness, do not exclusively depends upon the amount of chemical bounds between the matrix and compatibilizer, but the synergistic behavior between morphology and interfacial adhesion.<sup>17–19</sup> In this specific case,

it was discussed that the formation of PA6-g-MMA-MA is favored in (PA6/MMA-MA)+ABS sequence. However, the larger amount of *grafted*-copolymer does not necessary leads to superior adhesion between both phases. This effect was clearly observed in rheological analysis shown in Figure 5 where complex viscosity ( $\eta^*$ ) and storage modulus ( $E'$ ) (ABS/MMA-MA)+PA6 are higher than the observed for (PA6/MMA-MA)+ABS, indicating a stronger interface due to the formation of an almost co-continuous structure, and consequently, a better compatibility. Thus, it is believed that the superior toughness of (ABS/MMA-MA)+PA6 is probably related to its almost co-continuous structure which resulted from the different mixture protocols. Such relation between co-continuity and toughness were reported in previous studies<sup>4,39</sup> and, in a pleasant way, guided us to an important interconnection between the selective dispersion of MMA-MA, morphological, thermomechanical, and mechanical properties.

## CONCLUSIONS

The PA6/ABS/MMA-MA system showed quite different behavior depending on blending sequence. In (ABS/MMA-MA)+PA6, compatibilizer is mostly located in the ABS phase, leading to the formation of an almost co-continuous structure. As reported in previous studies, co-continuity might be the main responsible for the superior toughness observed for this composition. However, despite its good mechanical properties, excessive amount of MMA-MA in ABS phase seems to hamper the thermomechanical resistance, resulting in low HDT values. On the other hand, in (PA6/MMA-MA)+ABS the MMA-MA is preferentially dispersed at polyamide matrix and the PA6-g-MMA-MA formation is apparently favored. When compatibilizer is mainly located in PA6, the negative effect in HDT is avoided; however, the enhancement in toughness is not as pronounced as observed in (ABS/MMA-MA)+PA6.

## ACKNOWLEDGMENTS

The authors would like to thank the São Paulo Research Foundation (FAPESP) for financially supporting this research under process number 2012/15445-5.

## REFERENCES

- Jang, S. P.; Kim, D. *Polym. Eng. Sci.* **2000**, *40*, 1635.
- Kudva, R. A.; Keskkula, H.; Paul, D. R. *Polymer* **2000**, *41*, 225.

3. Burgisi, G.; Paternoster, M.; Peduto, N.; Saraceno, A. *J. Appl. Polym. Sci.* **1997**, *66*, 777.
4. Ozkoc, G.; Bayram, G.; Bayramli, E. *J. Appl. Polym. Sci.* **2007**, *104*, 926.
5. Huang, J. J.; Keskkula, H.; Paul, D. R. *Polymer* **2004**, *45*, 4203.
6. Tanrattanakul, V.; Sungthong, N.; Raksa, P. *Polym. Test.* **2008**, *27*, 794.
7. Bhattacharyya, A. R.; Maiti, S. N.; Misra, A. *J. Appl. Polym. Sci.* **2002**, *85*, 1593.
8. Wu, C. J.; Kuo, J. F.; Chen, C. Y. *Polym. Eng. Sci.* **1993**, *33*, 1329.
9. Ke, Z.; Shi, D.; Yin, J.; Li, R. K. Y.; Mai, Y. W. *Macromolecules* **2008**, *41*, 7264.
10. Kudva, R. A.; Keskkula, H.; Paul, D. R. *Polymer* **1998**, *39*, 2447.
11. Mojarrad, A.; Jahani, Y.; Barikani, M. *J. Appl. Polym. Sci.* **2011**, *120*, 2173.
12. Jafari, S. H.; Pötschke, P.; Stephan, M.; Warth, H.; Alberts, H. *Polymer* **2002**, *43*, 6985.
13. Kim, B. K.; Lee, Y. M.; Jeong, H. M. *Polymer* **1993**, *34*, 2075.
14. Triacca, V. J.; Ziaee, S.; Barlow, J. W.; Keskkula, H.; Paul, D. R. *Polymer* **1991**, *32*, 1401.
15. Dagli, S. S.; Kamdar, K. M. *Polym. Eng. Sci.* **1994**, *34*, 1709.
16. Araújo, E. M.; Hage, E.; Carvalho, A. J. F. *J. Mater. Sci.* **2005**, *40*, 4239.
17. Kim, J. K.; Kim, S.; Park, C. E. *Polymer* **1997**, *38*, 2155.
18. Díaz, M. F.; Barbosa, S. E.; Capiati, N. *J. Polymer* **2005**, *46*, 6096.
19. Sung, Y.; Han, M.; Hyun, J.; Kim, W.; Lee, H. *Polymer* **2003**, *44*, 1681.
20. Araújo, E. M.; Hage, E.; Carvalho, A. J. F. *J. Mater. Sci.* **2003**, *38*, 3515.
21. Hale, W.; Keskkula, H.; Paul, D. R. *Polymer* **1999**, *40*, 365.
22. Wang, Q.; Zhu, J.; Wang, P.; Li, L.; Yang, Q.; Huang, Y. *J. Appl. Polym. Sci.* **2012**, *124*, 5064.
23. Ha, M. H.; Kim, M. S.; Kim, B. K.; Kim, W.; Lee, M. C.; Kim, H. D. *J. Appl. Polym. Sci.* **2004**, *92*, 804.
24. Hale, W.; Keskkula, H.; Paul, D. R. *Polymer* **1999**, *40*, 3665.
25. Becker, D.; Hage, E.; Pessan, L. A. *J. Appl. Polym. Sci.* **2010**, *115*, 2540.
26. Spridon, D.; Panaitescu, L.; Ursu, D.; Uglea, C. V. *Polym. Int.* **1997**, *43*, 175.
27. Kusmono, Mohd Ishak, Z. A.; Chow, W. S.; Takeichi, T. R. *Eur. Polym. J.* **2008**, *44*, 1023.
28. Stewart, M. E.; George, S. E.; Miller, R. L.; Paul, D. R. *Polym. Eng. Sci.* **1993**, *33*, 675.
29. Larocca, N. M.; Hage, E.; Pessan, L. A. *J. Polym. Sci. Part B: Polym. Phys.* **2005**, *43*, 1244.
30. Oshinski, A. J.; Keskkula, H.; Paul, D. R. *Polymer* **1992**, *33*, 284.
31. Sundararaj, U.; Macosko, C. W. *Macromolecules* **1995**, *28*, 2647.
32. Lyu, S.; Jones, T. D.; Bates, F. S.; Macosko, C. W. *Macromolecules* **2002**, *35*, 7845.
33. Wildes, G.; Keskkula, H.; Paul, D. R. *J. Polym. Sci. Part B: Polym. Phys.* **1999**, *37*, 71.
34. Paul, D. R.; Barlow, J. W. *J. Macromol. Sci. Part C* **1980**, *18*, 109.
35. As'Habi, L.; Jafari, S. H.; Khonakdar, H. A.; Baghaei, B. *J. Polym. Res* **2011**, *18*, 197.
36. Devaux, E.; Bourbigot, S.; ElAchari, A. *J. Appl. Polym. Sci.* **2002**, *86*, 2416.
37. Bhardwaj, I. S.; Kumar, V.; Mathur, A. B.; Das, A. *J. Therm. Anal.* **1990**, *36*, 2339.
38. Chiu, F. C.; Lai, S. M.; Chen, Y. L.; Lee, T. H. *Polymer* **2005**, *46*, 11600.
39. Oliveira, A. D.; Larocca, N. M.; Paul, D. R.; Pessan, L. A. *Polym. Eng. Sci.* **2012**, *52*, 1909.
40. Kudva, R.; Keskkula, H.; Paul, D. R. *Polymer* **1999**, *40*, 6003.
41. Majumdar, B.; Keskkula, H.; Paul, D. *Polymer* **1994**, *35*, 3164.